International Scholarly Research Network
ISRN Optics
Volume 2012, Article ID 373968, 6 pages
doi:10.5402/2012/373968

Research Article

Photonic Eigenmodes in a Photonic Crystal Membrane

E. Ya. Glushko,[1] O. E. Glushko,[1,2] and L. A. Karachevtseva[1]

[1] *Institute of Semiconductor Physics of NAS of Ukraine, Nauki Prsp., 45, 03028 Kiev, Ukraine*
[2] *Institute of Physics, University of Leoben, Franz Josef Straße 18, 8700 Leoben, Austria*

Correspondence should be addressed to E. Ya. Glushko, eugene.glushko@scientist.com

Received 24 November 2011; Accepted 21 December 2011

Academic Editors: K. Hane and S. R. Restaino

Photonic membranes are the most widely used kind of 2D photonic crystals in signal processing. Nevertheless, some important aspects of electromagnetic field behavior in membrane like photonic crystals (MPCs) need detail investigation. We develop the approach close to resonant coupling modes method which unites both external and intrinsic problems, in-plane and out-of-plane geometries, and resonator properties of MPC. The resonator standing modes are excited by an external source through the special inputs and may be controlled due to the nonlinear coating. Typical photonic manifestations are studied for Si/SiO_2 2D membrane resonators of rectangular.

1. Introduction

Usually, membranes perform the task of separation during the process of selective transport of particles of a matter through the membrane channels. In photonics, the membranes are a kind of 2D photonic crystals which may be characterized as thin and wide systems ordered in both transversal directions and filtering radiation along the normal to surface direction. Many examples of membrane usage in photonics are discussed in the literature beginning from mechanical usage in mirrors and actuators [1–3] and up to laser applications. Photonic membranes transmit and reflect incident light uniting diffractional out-of-plane phenomena and the in-plane geometry interference phenomena caused by complicated inner structure of the membrane. The membrane peculiarities in reflected light angular distribution in grating spectra were well known long ago beginning with R. Wood's work [4]. Recently, the photonic bandgap manifestations in the reflectivity of periodically patterned systems were investigated experimentally and theoretically in [5–8] using a novel resonant coupling wave method (RCWM) connecting photonic bands existing for in-plane geometry of incidence with both diffractional signals in reflection and transmission. In [9] sharp resonances in the optical transmission spectra at normal incidence were observed for high-quality chalcogenide photonic crystal membranes and associated with Fano coupling between free space and the membrane-guided modes. It was shown in [9] that the membrane-guided modes near the centre of the first Brillouin zone are responsible for the main spectral features. An overview of silicon-based photonic crystals is presented in [10]. Optical effects in the thin-film 2D photonic crystals were overviewed in [11]. The gratings on thin silicon membranes fabricated in [12] exhibit clearly expressed resonant behaviour of responses that gives an opportunity for narrow bandwidth filtering applications. In [13], reported were the silica-embedded silicon photonic crystal waveguides offered an alternative to air-channelled membranes which are fully compatible with the monolithic integration. The authors show that despite the reduced refractive index contrast compared to the air membranes, the considered structures offer an operating area near the technologically important 1550 nm window. More complicated spiral structure was fabricated and investigated in [14], where optical properties of the three-dimensional silicon square spiral photonic crystal were considered. In [15], the extremely high-Q channels in a two-dimensional photonic crystal membrane were investigated. The controlled interaction between the membrane and a glass fiber tip in the near field of the photonic crystal was used to build a complete spatiospectral

map of the channel resonator mode and its coupling with the fiber tip. The near-field imaging and frequency tuning of a high-Q photonic crystal membrane was investigated in [16] as well. In [17], the ultralow loss photonic circuit based on waveguides integrated into the membrane-type photonic crystal. The transmission characteristics of the system were measured and record low propagation losses in photonic crystal waveguides of were obtained. Lasing spectrum of the GaInAsP/InP membrane laser and simulated resonant spectra for a few orders of transverse modes were obtained in [18], where a room-temperature continuous-wave operation under optical pumping was demonstrated and the threshold pump power characteristics were investigated.

The existing terminology concerning photonic crystals (PhCr), photonic membranes, and photonic resonators may be expressed in the following way. The infinite 2D structures ordered in XY plane which has also infinite size in Z direction may be called the photonic crystal. The photonic crystal resonator is a finite 2D system with perfectly smooth side walls. This detail leads to a clear expressed angular area of total internal reflection (Figure 1, yellow lines) for field closed inside the resonator. In ideal case, the system should have infinite size in Z direction. The only way to excite intrinsic standing waves is to use the input prisms due to that the external beam may hit into the total internal reflection area. The photonic membrane may be treated as a thin photonic crystal and in this capacity it exhibits properties of a two-dimensional system. The transformation from a photonic membrane to the photonic membrane resonator transforms the initial 2D system into a 3D system.

In this work, we consider a development of the existing calculation method RCWM to solve the external problem for electromagnetic field in space divided by the 2D membrane-type photonic crystal into two half-spaces. The Standing Wave Expansion (SWE) method in finite 2D structures is developed for in-plane geometry of incidence. The spectrum of modes trapped inside the total internal region of the Si/SiO_2 photonic resonator is calculated in 0-approximation of SWE method. In out-of-plane geometry, light reflection and transmission are investigated in chosen geometry of incidence taking into account the existing in-plane modes.

2. In-Plane Geometry: SWE Theory for Electromagnetic Field in a Finite 2D Photonic Crystal

The SWE method uses a special way of expansion by analytically found eigenstates of two probe finite 1D photonic crystals. In SWE, the eigenvalue problem is solved separately for two crossed perpendicularly 1D probe photonic crystals and resulting 0-approximation 2D basis is obtained as a direct production of separated bases. In considered case of p-polarization, the most convenient basis of functions may be built on the modes magnetic field. The mode magnetic field spatial dependence was found in [19–22]. For example,

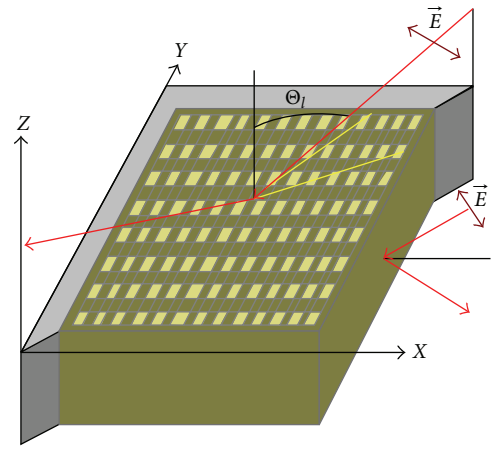

Figure 1: XY section of a finite 8×13 2D membrane. Out-of-plane incidence: s-polarization, Θ_l, external polar angle of incidence, azimuth angle $\Phi_l = \pi/4$; yellow (light gray) lines, sector of total internal reflection. In-plane incidence: p-polarization. The input prism is not shown. Material 1, system matrix; material 2, rectangular bars in matrix; material 3, covering layer, external medium is shown by grey.

inside a PhCr resonator for magnetic field in an arbitrary ij area we have 0-approximation expression for mode function:

$$\vec{H}_{ij}^{sg}(x,y) = \vec{e}_z \frac{2 \cdot F_i \cos(k_{is}x + \psi_{is})}{(n_i \sin\theta_i)} \cdot \frac{2 \cdot G_j \cos\left(k_{jg}y + \psi_{jg}\right)}{\left(n_j \sin\theta_j\right)} = |s,g\rangle, \tag{1}$$

where $n_{i,j}$ denotes refraction index in matter of photonic crystal area i or $j \cdot s$, g enumerate the probe 1D states. F_i, G_j are analytically obtained 1D mode amplitudes inside intrinsic areas $j, i = 1, \ldots, 2N+1$, whereas for outside areas where $i = 0$ or $j = 0$ cosines should transfer into $\exp(-k_{is}x)$ or $\exp(-k_{jg}y)$, correspondingly. ψ_{is}, ψ_{jg} are analytically obtained phases in framework of 1D problem for two probe crossed photonic crystals. The wavefront orientation with respect to OX axes is given by angle $\theta_i = \theta_1$ or θ_2 for odd or even layers of a probe 1D PhCr with appropriate geometry [19]. The angles θ_j present in y-part of the basis function are $\pi/2 - \theta_1$ or $\pi/2 - \theta_2$ for odd or even layers, respectively. Here, the index 1 corresponds to the topologically connected matrix material 1, and index 2 denotes the embedded into the matrix ordered bars of material 2. Below, we study the rectangular photonic crystal resonator based on a 2D terminated binary structure consisting of the topologically connected matrix material and another one-disconnected material 2 which looks like a system of rectangular bars.

The considered medium is sectionally continued with respect to optical density. Therefore, the dielectric function $\varepsilon(x,y)$ may be carried through the derivative and we have the wave equation

$$\frac{1}{\varepsilon(x,y)}\Delta H + \frac{\omega^2}{c^2}H = 0, \tag{2}$$

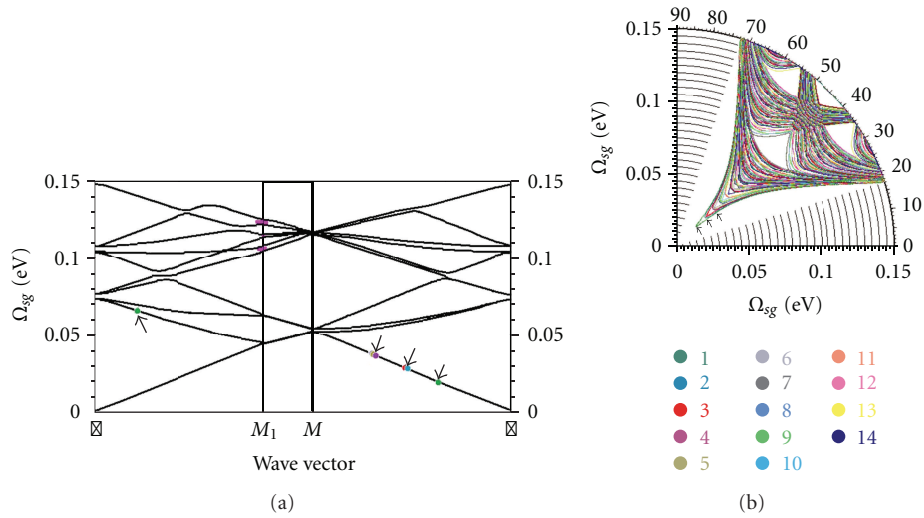

Figure 2: Comparison of results for finite and infinite 2D structures. Symmetry is shown in Figure 1. Elementary cell parameters: $d_{1x} = d_{1y} = 4\,\mu$m, $d_{2x} = d_{2y} = 1\,\mu$m. (a) Plane wave calculation for infinite Si/SiO$_2$ photonic crystal. ΓM, diagonal $\theta_1 = 45^\circ$ direction, ΓM_1, $\theta_1 = 33.69^\circ$ direction. Six lowest resonator modes are shown by corresponding colour points, beginning with $\Omega_{\min} \approx 0.0197$ eV (arrows). Three lowest gaps are shown along M_1 vertical line. (b) Modes of the 8×8 Si/SiO$_2$ 2D rectangular lattice resonator. Angular mode diagram. Calculated by the SWE method 0-approach modes allocated in the polar diagram. Shown are 901 lowest energy existing branches in 14 colour gradation inside the total internal reflection area, energy interval (0, 0.15) eV, angular interval $17.1^\circ < \theta_1 < 72.9^\circ$, lattice period 5.0 μm. The corresponding lowest modes along ΓM direction are marked by arrows.

for OZ-oriented magnetic field in the resonator. It should be taken into account that 2D basis $|s,g\rangle$ is composed from two separate 1D bases taken at angles θ and $\pi/2 - \theta$: $|s,g\rangle_{xy} = |s(\theta)\rangle_x \cdot |g(\pi/2-\theta)\rangle_y$. The expansion into the series gives

$$H = \sum_{s,g} h_{sg} \cdot |s,g\rangle. \tag{3}$$

Then, (3) generates the system of equations for expansion amplitudes h_{sg}:

$$\begin{cases} \displaystyle\sum_{s,g}\left[\langle q|\frac{k_{sg}^2}{\varepsilon(x,y)}|sg\rangle - \frac{\Omega^2}{c^2}\delta_{q,sg}\right]h_{sg}, \\ q = 1,\ldots,N_m, \end{cases} \tag{4}$$

where q numbers states of the 2D basis, matrix elements $\langle q|k_{sg}^2/\varepsilon(x,y)|s,g\rangle$ mean the integral over the resonator. It should be noted that matrix elements have the analytical form in our approach as the field H is described by amplitudes $F(s,i)$, $G(g,j)$ and phases ψ_{is}, ψ_{is} found in 1D problem which play part of the 2D basis generator. The full solution is given by a multitude of eigenvalues and corresponding standing waves or resonator modes:

$$\left\{\Omega_q^2, \begin{pmatrix} h_1^q \\ \vdots \\ h_{N_m}^q \end{pmatrix}\right\}, \tag{5}$$

where q enumerates 2D states which are standing waves inside the total internal reflection area of the resonator, h_m^q are coefficients of the 2D state q expansion into initial basis $|s,g\rangle$ series. First, the SWE method calculation of the bandgap structure was performed for a low contrast CdSe/CdS photonic resonator in [23].

In this paper, we consider a more contrast system—a Si/SiO$_2$ resonator of rectangular form which has 8×8 periods plus one external layer of material 3 (Figure 1). Also, the calculation was performed for an infinite Si/SiO$_2$ photonic crystal with the same symmetry by using the plane wave expansion method. The PhCr lattice has the rectangular symmetry (Figure 1), and bars of material 2 have also rectangular form: $d_{2x} = d_{2y} = 1.0\,\mu$m and for material 1 voids $d_{1x} = d_{1y} = 4\,\mu$m. In Figure 2(a), the results calculated for the direction of symmetry ΓM and nonsymmetry directions $k_x = 1.5k_y$ ΓM_1 and MM_1 are shown. The calculation shows that gaps exist only along the ΓM_1 direction. Three lowest gaps are shown by arrows along the M_1 vertical line: between fourth-fifth (of width 0.025 eV), sixth-seventh (0.012 eV), and ninth-tenth (0.030 eV) Brillouin zones in the extended scheme. The resonator property to trap the wave inside is exhibited in the angular area near the diagonal $\theta_1 = \pi/4$ direction (ΓM). Six lowest trapped modes taken from SWE calculation for a finite resonator are plotted at the ΓM branch (colour points). In Figure 2(b), the mode structure calculated in 0-approximation of SWE [20] for a finite PhCr resonator is shown in polar coordinate system for the first 901 standing waves with accuracy $\approx$ 0.001. The energy interval (0, 0.15) eV, the alternating 2D mode branches are shown in 14-colour scale. The mode branches in the total internal reflection area (Θ_{total}, $\pi/2 - \Theta_{\text{total}}$) of the resonator under study are allocated symmetrically near the bisector $\theta_1 = \pi/4$ and they are doubly degenerated due to the rectangular symmetry of the system. The same above-mentioned lowest resonator modes are marked by

arrows beginning with $\Omega_{\min} \approx 0.02$ eV (Figure 2(b)). When N increase to infinity then $\Omega_{\min} \to 0$. The direction ΓM_1 ($\theta_1 = 33.69^\circ$) in the resonator contains a gap in area of low frequencies, and the band of states begins with $\Omega_{\min} \approx 0.065$ eV. It is caused by the fact that each wave propagating inside the resonator at an arbitrary angle θ is mixing by the resonator with the $(\pi/2 - \theta)$ wave that makes the selection rule for permitted standing waves more rigid. Therefore, the states existing in an infinite PhCr may be forbidden in a resonator: the first permitted resonator state arises for the ΓM_1 direction at 0.065 eV and is situated on the second photonic branch in the scheme of reduced zones shown in Figure 2(a) (left arrow).

Our SWE calculations give a smooth transformation of the considered 2D mode structure from 2D structure shown in Figure 2(b) to the 1D one shown in Figure 3 if d_{1y} or d_{2y} increase in accordance with real transformation of a 2D resonator into a 1D one. The spectrum has the discrete character due to finite size of the resonator. Instead of the continuous multitude of electromagnetic eigenstates distributed along the modal surface, we have got several angle-depended mode lines. To compare the results obtained for 1D and 2D systems we have studied two 1D structures which have close parameters d_1 and d_2 and may be considered in some sense as a parent structure for the considered above 2D resonator [20]. The modes of the 1D 8-period Si/SiO_2 resonator calculated by the transfer matrix method are shown in Figure 3 for the resonator total internal reflection area $17.1^\circ < \theta_{\text{total}} < 72.9^\circ$ in energy interval (0, 0.5) eV. Geometric parameters were taken close to that for considered above 2D system: matrix material layers $d_1 = 4.0\,\mu$m, layer thickness $d_2 = 1.0\,\mu$m (glass layers). The material of covering layer was taken coinciding with the matrix: material 3 = material 1 both for 2D resonator and 1D PhCr. Due to the considerable optical contrast of the binary system under consideration the waveguide-type [23] angular area is present (shown by red), and the band states belonging to the transmitted type are shown by violet. The angular boundary between these two types of states passes at $\theta_1 \approx 26.2^\circ$. The lowest 1D state at $\theta_1 = \pi/4$ is $\omega_{\min} \approx 0.014$ eV that to average $\Omega_{\min} \approx \sqrt{2}\omega_{\min}$ [20]. The considerable gaps arise far inside the total internal reflection area. Local or surface modes detached from bands in transmitted and waveguide areas are shown by blue and light blue. Upper restriction 1.272 rad chosen for angular area is caused by the demand $\pi/2 - \Theta_{\text{total}}$ which is important for 2D resonators of chosen geometry.

Below we will consider the method to solve the united external-intrinsic problem for a finite 2D photonic crystal membrane.

3. Uniting In-Plane and Out-of-Plane Geometries: The In-plane Modes Contribution Into Reflection

The typical geometry of an external problem for a limited 2D membrane is shown in Figure 1. Two principally different angular areas exist for external incidence. First is when the

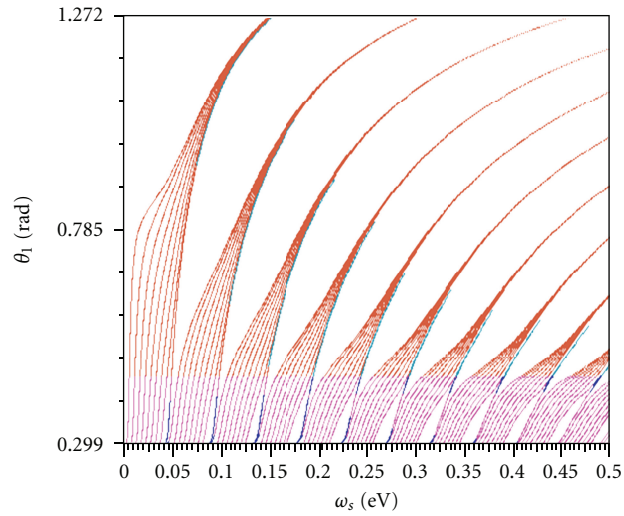

Figure 3: The modes of a 1D 8 period Si/SiO_2 resonator calculated in the transfer matrix method. Shown are lowest existing branches in the total internal reflection area $17.1^\circ < \theta_{\text{total}} < 72.9^\circ$ of the resonator. Extended waves (area $17.1^\circ < \theta_1 < 26.2^\circ$) are shown by violet, waveguide-type waves ($\theta_1 > 26.2^\circ$ are shown by red, detached local (surface) modes are shown by blue and light blue (waveguide area). Energy interval (0, 0.5) eV, s enumerates 1D modes, layer thickness: $d_1 = 4.0\,\mu$m $d_2 = 1.0\,\mu$m (glass layers).

beam hits into the sector of standing waves between the two yellow lines inside the total internal reflection of the resonator. For these directions, the membrane may be treated as an effective medium where the external wave excites the eigenmodes of the resonator. Another case arises for all directions of incidence outside the sector shown in Figure 1, and the incident wave excites extended waves in the membrane instead of eigenmodes.

We concentrate our efforts on the first regime of out-of-plane incidence when azimuth angle is taken $\Phi_l = \pi/4$ (Figure 1, bisector plane). Under consideration is the s-polarized wave incident at the angle Θ_l on the top surface of the membrane. Inside the resonator, this wave excites standing waves (resonator eigenmodes) which have the character of pure p-polarized waves. In the lower semispace field transforms into s-polarized wave again.

The SWE method gives the full solution (5) for p-polarized field inside the resonator. In terms of effective medium the solution (5) determines totally the optical characteristics of the membrane which divides total space into upper semispace and the lower one. The given frequency of incident wave ω mixes with the in-plane discrete spectrum Ω_q and produces z-component of field inside the membrane:

$$k_z = \frac{\sqrt{\omega^2 - \Omega_q^2}}{c}. \tag{6}$$

The wave vector projection k_z becomes imaginary for low frequency incident waves, and, therefore, z-component of field has only decaying tails inside the PCM under consideration. If wave frequencies ω become higher than Ω_q, a line of interference peaks should arise which is caused by

field resonance in the perpendicular to the film direction. The two-wave solution for electromagnetic field may be represented by means of the magnetic field in all three media

$$n_a\vec{H}_a = (n_{az}, -n_{ax})A_a e^{ik_{az}z} - (n_{az}, n_{ax})B_a e^{-ik_{az}z}, \quad (7)$$

where $a = \{l, m, r\}$ denotes upper half-space, membrane, and lower half-space, respectively. The amplitude B_r for the lower half space should be taken equal to zero.

Further, boundary conditions of continuity for magnetic field at both surfaces $z = 0$ and $z = L$ lead to the system of equations for unknown amplitudes. In matrix view we have

$$\begin{bmatrix} -h_{lx} & h_{mx} & h_{mx} & 0 \\ h_{lz} & -h_{mz} & h_{mz} & 0 \\ 0 & \tilde{h}_{mx} & \tilde{h}^*_{mx} & -h_{rx} \\ 0 & \tilde{h}_{mz} & -\tilde{h}^*_{mz} & h_{rz} \end{bmatrix} \begin{bmatrix} B_{\mathrm{l}} \\ A_{\mathrm{m}} \\ B_{\mathrm{m}} \\ A_{\mathrm{r}} \end{bmatrix} = A_l \begin{bmatrix} h_{lx} \\ h_{lz} \\ 0 \\ 0 \end{bmatrix}, \quad (8)$$

where for all indices a shorthand notations are made $h_{ax} = n_{ax}/n_a$, $h_{az} = n_{az}/n_a$, and $\tilde{h}_{ax,z} = h_{ax,z}e^{ik_{az}z}$. Equation (8) determines contribution in amplitudes A_r^q and B_l^q of field caused by a separate intrinsic mode q. For an optically linear system, the result may be expressed as a weighed sum taken over the basis of eigenmodes q. Therefore, supposing $A_l = 1$, we have for reflection and transmission

$$R = \frac{1}{M}\sum_{q=1}^{M}\left|B_l^q\right|^2, \qquad T = \frac{1}{M}\sum_{q=1}^{M}\left|A_r^q\right|^2, \quad (9)$$

where M is basis length and q enumerates ordered 2D basis functions $|q\rangle$ calculated in SWE method at given azimuth angle Φ_l. In previous section, we calculate 2D spectrum of intrinsic modes for in-plane geometry of incidence (Figures 1 and 3(b)) at $\Phi_l = \pi/4$. For this bisect direction, it begins starting from 0.0197 eV and includes 901 states in energy interval (0, 0.15) eV. In Figure 4, the transmission versus frequency dependence for a thin PhCr membrane $L = 50\,\mu$m is shown for five Φ_l values in interval beginning with the almost normal incidence angle 6 grad and up to 54 grad. For all angles of incidence, the every dense group of modal states (Figure 4, bar graph 1) contributes to the transmission increase. Much less increasing or even drop is observed in the frequency regions between the peaks of the DOS. Light interference caused by the membrane effective medium exhibits itself in area of energies beginning with 0.15 eV as small beating on the envelope dependence of transmission. Further, they became more clearly expressed beginning with 0.4 eV. Depending on the membrane thickness, the density of resonances may be lesser or higher. The transmission dependence for a thick PCM $L = 100\,\mu$m exhibits twice higher density of resonances beginning with 0.4 eV than density shown in Figure 4. For a thick PCM, at each angle of incidence Θ_l the big density of resonances creates the envelope line showing results close to that may be obtained for a nonperfect thick 2D photonic macroporous silicon structure [24]. A more detailed analysis of resonances nature will be made elsewhere. In the inset (Figure 4), the contribution of a solitary phonon polariton mode

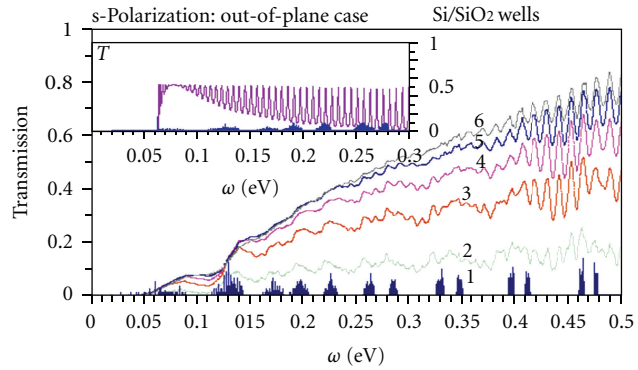

Figure 4: Contribution of resonator's modes into the light transmission through the membrane. SWE and coupled wave method calculation for finite 8×8 Si/SiO$_2$ photonic membrane. Contribution of resonator's modes $\Omega_q > 0.02$. Incidence in the diagonal $\theta_1 = \pi/4$ (ΓM) direction. Elementary cell parameters: $d_{1x} = d_{1y} = 4\,\mu$m, $d_{2x} = d_{2y} = 1\,\mu$m. Shown is transmission in energy interval (0, 0.5) eV. 1, normalized DOS diagram. Angles of incidence. 2: $\Theta_l = 6°$; 3: $\Theta_l = 18°$; 4: $\Theta_l = 30°$; 5: $\Theta_l = 42°$; 6: $\Theta_l = 54°$. The membrane thickness, $L = 50\,\mu$m. Inset: contribution of the phonon polariton mode $\Omega_{\mathrm{ph}} = 0.0629$ eV, $L = 100\,\mu$m, $\Theta_l = 36°$.

$\Omega_{\mathrm{ph}} = 0.0629$ eV, $\Theta_l = 36°$ added with weight number = 2000 to the found 901 pure electromagnetic modes is plotted.

In considered approach, the photonic crystal membrane is treating in spirit of an effective medium describing by a multitude of in-plane resonant eigenmodes. Another (nonresonator) case arises if azimuth angle Φ_l lies outside the sector of total internal reflection area of the resonator. Therefore, this case needs another approach which will be considered in another work. It should be noted that in the SWE method developed in present paper the information about direction of initial waves remains in modal numbers. Second, the expansion procedure in SWE is carried out by standing waves which have practically zero amplitudes outside the resonator.

4. Summary

Here, we develop the approach uniting both external and intrinsic problems, in-plane and out-of-plane geometries, and resonator properties of PCM. The resonator in-plane standing modes can be excited by an external source through the special inputs and may be controlled due to their nonlinear properties. Also, we have considered light transmission in out-of-plane geometry for rectangular 2D photonic membrane resonators where the incident wave may excite the trapped standing modes. Finally, it should be noted that the proposed SWE method for finite resonators uses open boundary conditions and may be adapted for any symmetry of the lattice as well as for any shape of material 2 bars in matrix material.

References

[1] D. K. Marker and C. H. Jenkins, "Surface precision of optical membranes with curvature," *Optics Express*, vol. 1, no. 11, pp. 324–331, 1997.

[2] H. M. Dyson, R. M. Sharples, N. A. Dipper, and G. V. Vdovin, "Cryogenic wavefront correction using membrane deformable mirrors," *Optics Express*, vol. 8, no. 1, pp. 17–26, 2001.

[3] C. Paterson, I. Munro, and J. C. Dainty, "A low cost adaptive optics system using a membrane mirror," *Optics Express*, vol. 6, no. 9, pp. 175–185, 2000.

[4] R. W. Wood, "On a remarkable case of uneven distribution of light in a diffraction grating spectrum," *Philysophical Magazine*, vol. 4, pp. 396–402, 1902.

[5] V. N. Astratov, D. M. Whittaker, I. S. Culshaw et al., "Photonic band-structure effects in the reflectivity of periodically patterned waveguides," *Physical Review B*, vol. 60, no. 24, pp. R16255–R16258, 1999.

[6] V. N. Astratov, I. S. Culshaw, R. M. Stevenson et al., "Resonant coupling of near-infrared radiation to photonic band structure waveguides," *Journal of Lightwave Technology*, vol. 17, no. 11, pp. 2050–2057, 1999.

[7] D. Cassagne, C. Jouanin, and D. Bertho, "Hexagonal photonic-band-gap structures," *Physical Review B*, vol. 53, no. 11, pp. 7134–7142, 1996.

[8] V. M. Fitio and Y. V. Bobitski, "Diffraction analysis by periodic structures using a method of coupled waves," *Opto-Electronics Review*, vol. 13, no. 4, pp. 331–339, 2005.

[9] C. Grillet, D. Freeman, B. Luther-Davies et al., "Characterization and modeling of Fano resonances in chalcogenide photonic crystal membranes," *Optics Express*, vol. 14, no. 1, pp. 369–376, 2006.

[10] A. Birner, R. B. Wehrspohn, U. M. Gösele, and K. Busch, "Silicon-based photonic crystals," *Advanced Materials*, vol. 13, no. 6, pp. 377–388, 2001.

[11] M. Kellegoz, I. Ozkan, and M. S. Kilickaya, "Performance effects of proton exchange membrane fuel cell at various operating temperatures," *Journal of Optoelectronics and Advanced Materials*, vol. 10, no. 2, pp. 369–372, 2008.

[12] Y. Wang, Y. Kanamori, J. Ye, H. Sameshima, and K. Hane, "Fabrication and characterization of nanoscale resonant gratings on thin silicon membrane," *Optics Express*, vol. 17, no. 7, pp. 4938–4943, 2009.

[13] T. P. White, L. O'Faolain, J. Li, L. C. Andreani, and T. F. Krauss, "Silica-embedded silicon photonic crystal waveguides," *Optics Express*, vol. 16, no. 21, pp. 17076–17081, 2008.

[14] S. R. Kennedy, M. J. Brett, H. Miguez, O. Toader, and S. John, "Optical properties of a three-dimensional silicon square spiral photonic crystal," *Photonics and Nanostructures*, vol. 1, no. 1, pp. 37–42, 2003.

[15] K. H. Hwang and G. H. Song, "Design of a high-Q channel add-drop multiplexer based on the two-dimensional photonic-crystal membrane structure," *Optics Express*, vol. 13, no. 6, pp. 1948–1957, 2005.

[16] S. Mujumdar, A. F. Koenderink, T. Sünner et al., "Near-field imaging and frequency tuning of a high Q photonic crystal membrane microcavity," *Optics Express*, vol. 15, no. 25, pp. 17214–17220, 2007.

[17] S. J. McNab, N. Moll, and Y. A. Vlasov, "Ultra-low loss photonic integrated circuit with membrane-type photonic crystal waveguides," *Optics Express*, vol. 11, no. 22, pp. 2927–2939, 2003.

[18] T. Maruyama, T. Okumura, S. Sakamoto, K. Miura, Y. Nishimoto, and S. Arai, "GaInAsP/InP membrane BH-DFB lasers directly bonded on SOI substrate," *Optics Express*, vol. 14, no. 18, pp. 8184–8188, 2006.

[19] E. Y. Glushko, "Switching of electromagnetic eigenwaves in metastructures," in *Photonic Crystal Materials and Devices*, vol. 6989 of *Proceedings of SPIE*, 2008.

[20] E. Y. Glushko, A. E. Glushko, V. N. Evteev, and A. N. Stepanyuk, "Electromagnetic eigenwaves in metastructures: perturbation theory method," in *Nanophotonics II*, vol. 6988 of *Proceedings of SPIE*, p. 118, 2008.

[21] E. Ya. Glushko, "All-optical signal processing in photonic structures with nonlinearity," *Optics Communications*, vol. 247, no. 4–6, pp. 275–280, 2005.

[22] E. Ya. Glushko, *Optics Express 18*, p. 3071, 2010.

[23] E. Y. Glushko, A. E. Glushko, V. N. Evteev, and A. N. Stepanyuk, "All-optical signal processing based on trapped modes of a photonic crystal resonator," in *3rd Nonlinear Optics and Applications*, vol. 7354 of *Proceedings of SPIE*, 2009.

[24] L. A. Karachevtseva, O. O. Lytvynenko, E. O. Malovichko, O. J. Stronska, E. V. Busaneva, and O. D. Gorchinsky, "Optical transmittance of 2D macroporous silicon structures," *Semiconductor Physics*, vol. 4, no. 4, pp. 347–351, 2001.